

# World Journal of *Stem Cells*

*World J Stem Cells* 2024 February 26; 16(2): 54-227



**EDITORIAL**

- 54 Human dental pulp stem/stromal cells in clinical practice  
*Grawish ME*
- 58 Multiple pretreatments can effectively improve the functionality of mesenchymal stem cells  
*Wan XX, Hu XM, Xiong K*
- 64 Cellular preconditioning and mesenchymal stem cell ferroptosis  
*Zineldeen DH, Mushtaq M, Haider KH*

**REVIEW**

- 70 Therapeutic utility of human umbilical cord-derived mesenchymal stem cells-based approaches in pulmonary diseases: Recent advancements and prospects  
*Meng M, Zhang WW, Chen SF, Wang DR, Zhou CH*
- 89 Unlocking the versatile potential: Adipose-derived mesenchymal stem cells in ocular surface reconstruction and oculoplastics  
*Surico PL, Scarabosio A, Miotti G, Grando M, Salati C, Parodi PC, Spadea L, Zeppieri M*

**MINIREVIEWS**

- 102 Crosstalk between Wnt and bone morphogenetic protein signaling during osteogenic differentiation  
*Arya PN, Saranya I, Selvamurugan N*
- 114 Human pluripotent stem cell-derived kidney organoids: Current progress and challenges  
*Long HY, Qian ZP, Lan Q, Xu YJ, Da JJ, Yu FX, Zha Y*
- 126 Recent progress in hair follicle stem cell markers and their regulatory roles  
*Xing YZ, Guo HY, Xiang F, Li YH*
- 137 Advances in the differentiation of pluripotent stem cells into vascular cells  
*Jiao YC, Wang YX, Liu WZ, Xu JW, Zhao YY, Yan CZ, Liu FC*

**ORIGINAL ARTICLE****Basic Study**

- 151 Silencing of Jumonji domain-containing 1C inhibits the osteogenic differentiation of bone marrow mesenchymal stem cells *via* nuclear factor- $\kappa$ B signaling  
*Li JY, Wang TT, Ma L, Zhang Y, Zhu D*
- 163 Effects of different concentrations of nicotinamide on hematopoietic stem cells cultured *in vitro*  
*Ren Y, Cui YN, Wang HW*

- 176** High quality repair of osteochondral defects in rats using the extracellular matrix of antler stem cells  
*Wang YS, Chu WH, Zhai JJ, Wang WY, He ZM, Zhao QM, Li CY*
- 191** Extracellular vesicles derived from mesenchymal stem cells mediate extracellular matrix remodeling in osteoarthritis through the transport of microRNA-29a  
*Yang F, Xiong WQ, Li CZ, Wu MJ, Zhang XZ, Ran CX, Li ZH, Cui Y, Liu BY, Zhao DW*
- 207** VX-509 attenuates the stemness characteristics of colorectal cancer stem-like cells by regulating the epithelial-mesenchymal transition through Nodal/Smad2/3 signaling  
*Yuan Y, Zhang XF, Li YC, Chen HQ, Wen T, Zheng JL, Zhao ZY, Hu QY*

**ABOUT COVER**

Editorial Board Member of *World Journal of Stem Cells*, Khawaja Husnain Haider, PhD, Professor, Department of Basic Sciences, Sulaiman Al-Rajhi University, AlQaseem 52726, Saudi Arabia. kh.haider@gmail.com

**AIMS AND SCOPE**

The primary aim of *World Journal of Stem Cells (WJSC, World J Stem Cells)* is to provide scholars and readers from various fields of stem cells with a platform to publish high-quality basic and clinical research articles and communicate their research findings online. *WJSC* publishes articles reporting research results obtained in the field of stem cell biology and regenerative medicine, related to the wide range of stem cells including embryonic stem cells, germline stem cells, tissue-specific stem cells, adult stem cells, mesenchymal stromal cells, induced pluripotent stem cells, embryonal carcinoma stem cells, hemangioblasts, lymphoid progenitor cells, *etc.*

**INDEXING/ABSTRACTING**

The *WJSC* is now abstracted and indexed in Science Citation Index Expanded (SCIE, also known as SciSearch®), Journal Citation Reports/Science Edition, PubMed, PubMed Central, Scopus, Biological Abstracts, BIOSIS Previews, Reference Citation Analysis, China Science and Technology Journal Database, and Superstar Journals Database. The 2023 Edition of Journal Citation Reports® cites the 2022 impact factor (IF) for *WJSC* as 4.1; IF without journal self cites: 3.9; 5-year IF: 4.5; Journal Citation Indicator: 0.53; Ranking: 15 among 29 journals in cell and tissue engineering; Quartile category: Q3; Ranking: 99 among 191 journals in cell biology; and Quartile category: Q3. The *WJSC*'s CiteScore for 2022 is 8.0 and Scopus CiteScore rank 2022: Histology is 9/57; Genetics is 68/325; Genetics (clinical) is 19/90; Molecular Biology is 119/380; Cell Biology is 95/274.

**RESPONSIBLE EDITORS FOR THIS ISSUE**

Production Editor: *Xiang-Di Zhang*; Production Department Director: *Xu Guo*; Editorial Office Director: *Jia-Ru Fan*.

**NAME OF JOURNAL**

*World Journal of Stem Cells*

**ISSN**

ISSN 1948-0210 (online)

**LAUNCH DATE**

December 31, 2009

**FREQUENCY**

Monthly

**EDITORS-IN-CHIEF**

Shengwen Calvin Li, Carlo Ventura

**EDITORIAL BOARD MEMBERS**

<https://www.wjgnet.com/1948-0210/editorialboard.htm>

**PUBLICATION DATE**

February 26, 2024

**COPYRIGHT**

© 2024 Baishideng Publishing Group Inc

**INSTRUCTIONS TO AUTHORS**

<https://www.wjgnet.com/bpg/gerinfo/204>

**GUIDELINES FOR ETHICS DOCUMENTS**

<https://www.wjgnet.com/bpg/GerInfo/287>

**GUIDELINES FOR NON-NATIVE SPEAKERS OF ENGLISH**

<https://www.wjgnet.com/bpg/gerinfo/240>

**PUBLICATION ETHICS**

<https://www.wjgnet.com/bpg/GerInfo/288>

**PUBLICATION MISCONDUCT**

<https://www.wjgnet.com/bpg/gerinfo/208>

**ARTICLE PROCESSING CHARGE**

<https://www.wjgnet.com/bpg/gerinfo/242>

**STEPS FOR SUBMITTING MANUSCRIPTS**

<https://www.wjgnet.com/bpg/GerInfo/239>

**ONLINE SUBMISSION**

<https://www.f6publishing.com>

## Basic Study

# Extracellular vesicles derived from mesenchymal stem cells mediate extracellular matrix remodeling in osteoarthritis through the transport of microRNA-29a

Fan Yang, Wan-Qi Xiong, Chen-Zhi Li, Ming-Jian Wu, Xiu-Zhi Zhang, Chun-Xiao Ran, Zhen-Hao Li, Yan Cui, Bao-Yi Liu, De-Wei Zhao

**Specialty type:** Cell and tissue engineering

**Provenance and peer review:**

Unsolicited article; Externally peer reviewed.

**Peer-review model:** Single blind

**Peer-review report's scientific quality classification**

Grade A (Excellent): 0  
Grade B (Very good): B, B  
Grade C (Good): 0  
Grade D (Fair): 0  
Grade E (Poor): 0

**P-Reviewer:** Arufe MC, Spain;  
Maurya DK, India

**Received:** October 26, 2023

**Peer-review started:** October 26, 2023

**First decision:** November 9, 2023

**Revised:** November 18, 2023

**Accepted:** January 30, 2024

**Article in press:** January 30, 2024

**Published online:** February 26, 2024



Fan Yang, Wan-Qi Xiong, Chen-Zhi Li, Ming-Jian Wu, Xiu-Zhi Zhang, Chun-Xiao Ran, Zhen-Hao Li, Yan Cui, Bao-Yi Liu, De-Wei Zhao, Department of Orthopedics, Affiliated Zhongshan Hospital of Dalian University, Dalian 116001, Liaoning Province, China

**Corresponding author:** Bao-Yi Liu, PhD, Chief, Professor, Surgeon, Teacher, Department of Orthopedics, Affiliated Zhongshan Hospital of Dalian University, No. 6 Jiefang Street, Zhongshan District, Dalian 116001, Liaoning Province, China. [liubaoyi-513@163.com](mailto:liubaoyi-513@163.com)

## Abstract

### BACKGROUND

Knee osteoarthritis (KOA) is a common orthopedic condition with an uncertain etiology, possibly involving genetics and biomechanics. Factors like changes in chondrocyte microenvironment, oxidative stress, inflammation, and immune responses affect KOA development. Early-stage treatment options primarily target symptom relief. Mesenchymal stem cells (MSCs) show promise for treatment, despite challenges. Recent research highlights microRNAs (miRNAs) within MSC-released extracellular vesicles that can potentially promote cartilage regeneration and hinder KOA progression. This suggests exosomes (Exos) as a promising avenue for future treatment. While these findings emphasize the need for effective KOA progression management, further safety and efficacy validation for Exos is essential.

### AIM

To explore miR-29a's role in KOA, we'll create miR-29a-loaded vesicles, testing for early treatment in rat models.

### METHODS

Extraction of bone marrow MSC-derived extracellular vesicles, preparation of engineered vesicles loaded with miR-29a using ultrasonication, and identification using quantitative reverse transcription polymerase chain reaction; after establishing a rat model of KOA, rats were randomly divided into three groups: Blank control group injected with saline, normal extracellular vesicle group injected with normal extracellular vesicle suspension, and engineered extracellular vesicle group injected with engineered extracellular vesicle suspension. The three groups

were subjected to general behavioral observation analysis, imaging evaluation, gross histological observation evaluation, histological detection, and immunohistochemical detection to compare and evaluate the progress of various forms of arthritis.

## RESULTS

General behavioral observation results showed that the extracellular vesicle group and engineered extracellular vesicle group had better performance in all four indicators of pain, gait, joint mobility, and swelling compared to the blank control group. Additionally, the engineered extracellular vesicle group had better pain relief at 4 wk and better knee joint mobility at 8 wk compared to the normal extracellular vesicle group. Imaging examination results showed that the blank control group had the fastest progression of arthritis, the normal extracellular vesicle group had a relatively slower progression, and the engineered extracellular vesicle group had the slowest progression. Gross histological observation results showed that the blank control group had the most obvious signs of arthritis, the normal extracellular vesicle group showed signs of arthritis, and the engineered extracellular vesicle group showed no significant signs of arthritis. Using the Pelletier gross score evaluation, the engineered extracellular vesicle group had the slowest progression of arthritis. Results from two types of staining showed that the articular cartilage of rats in the normal extracellular vesicle and engineered extracellular vesicle groups was significantly better than that of the blank control group, and the engineered extracellular vesicle group had the best cartilage cell and joint surface condition. Immunohistochemical detection of type II collagen and proteoglycan showed that the extracellular matrix of cartilage cells in the normal extracellular vesicle and engineered extracellular vesicle groups was better than that of the blank control group. Compared to the normal extracellular vesicle group, the engineered extracellular vesicle group had a better regulatory effect on the extracellular matrix of cartilage cells.

## CONCLUSION

Engineered Exos loaded with miR-29a can exert anti-inflammatory effects and maintain extracellular matrix stability, thereby protecting articular cartilage, and slowing the progression of KOA.

**Key Words:** Exosomes; Osteoarthritis; Mesenchymal stem cells; MicroRNA-29a; Intra-articular injection

©The Author(s) 2024. Published by Baishideng Publishing Group Inc. All rights reserved.

**Core Tip:** Knee osteoarthritis (KOA) is a common orthopedic condition with an uncertain etiology, involving genetics and biomechanics. Factors like changes in chondrocyte microenvironment, oxidative stress, inflammation, and immune responses affect KOA. Mesenchymal stem cells (MSCs) show promise in treatment. Recent research highlights microRNAs (miRNAs) within MSC-released extracellular vesicles that can potentially promote cartilage regeneration and hinder KOA. Engineered exosomes (Exos) loaded with miR-29a were used in a rat study for early-stage KOA treatment, showing superior pain reduction and joint improvement compared to standard Exos. These findings suggest that miR-29a-loaded Exos could be a novel therapeutic approach for early-stage KOA management.

**Citation:** Yang F, Xiong WQ, Li CZ, Wu MJ, Zhang XZ, Ran CX, Li ZH, Cui Y, Liu BY, Zhao DW. Extracellular vesicles derived from mesenchymal stem cells mediate extracellular matrix remodeling in osteoarthritis through the transport of microRNA-29a. *World J Stem Cells* 2024; 16(2): 191-206

**URL:** <https://www.wjgnet.com/1948-0210/full/v16/i2/191.htm>

**DOI:** <https://dx.doi.org/10.4252/wjsc.v16.i2.191>

## INTRODUCTION

Knee osteoarthritis (KOA) is a common orthopedic disease that seriously affects the quality of life of patients and is a common clinical problem. The etiology of KOA is not fully understood, but it might be associated with genetic, biological, and biomechanical factors[1]. Aging and abnormal mechanical stress leading to changes in the microenvironment of chondrocytes are some of the mechanisms underlying KOA[2]. Pathological events, such as oxidative stress, synovial inflammation, and immune responses, also contribute to the development of KOA[3]. However, joint cartilage lacks vascular nutrition and self-repair ability, resulting in the loss of chondrocyte integrity and activity, which in turn accelerates cartilage degradation and damage[4-6]. Research indicates that KOA is one of the most common diseases in orthopedic clinical practice, accounting for approximately 40% of all types of arthritis[1]. Therefore, effective treatments and preventive measures need to be developed for managing KOA. Treatment options for KOA are limited, and the choice of treatment varies with the requirements of the patient. Patients in advanced stages may require surgical intervention, but it has the risk of functional impairment and prosthetic longevity. Non-surgical treatments, such as lifestyle modifications, physical therapy, and pharmacotherapy, are commonly used for treating patients with early-stage KOA[7-9]. However, pharmacotherapy recommended by international guidelines only provides symptomatic relief. It

has limited efficacy and shows considerable individual variation. Thus, effective treatment strategies need to be developed to delay the progression of KOA. While researchers seek drugs to treat KOA, their safety and efficacy need further validation[10,11]. Hence, safe and effective treatment methods are required to improve the condition of KOA.

Many researchers have investigated mesenchymal stem cells (MSCs) for their role in tissue repair and regeneration. They can promote chondrocyte matrix regeneration and inhibit inflammatory responses, and thus, may be used for tissue repair and regeneration. MSCs from different sources can inhibit the development of OA (KOA) by improving the cartilage matrix or suppressing related inflammatory factors, thus protecting the joint cartilage[12,13]. Specifically, bone marrow-derived MSCs (BMSCs) are multifunctional cells that have great potential in the treatment of various diseases, including KOA[14]. However, the application of MSCs faces multiple issues, such as ethical concerns, transplant rejection, and risk of tumor formation. Thus, further research is required to address these problems. Some studies have reported that the therapeutic efficacy of treating KOA with BMSCs is closely related to the exosomes (Exos) secreted by BMSCs [15]. Exos are extracellular vesicles released by almost all eukaryotic cells. They carry various substances, such as proteins, lipids, and RNA for cell communication. Many studies have shown that Exos contain various microRNAs (miRNAs), which can promote chondrocyte proliferation, cartilage matrix secretion, anti-inflammatory effects, and cartilage regeneration[16,17]. Through *in vitro* and *in vivo* experiments, researchers have demonstrated the potential of Exos in treating KOA and elucidated the mechanisms underlying the delay in the progression of KOA. However, natural Exos have some limitations, such as poor targeting ability, low quantity, and restricted payload capacity[18,19]. To address these issues, researchers have improved the targeting ability and loading capacity of Exos to enhance their therapeutic effects. Engineered Exos offer a new strategy for treating OA[20].

The small non-coding RNA molecule miR-29a is involved in various physiological and pathological processes in the human body, such as cell proliferation, differentiation, apoptosis, fibrosis, and angiogenesis[21]. Studies on miR-29a mainly investigated its function in areas such as tumors, thoracic surgery, obstetrics, and gynecology. Cui *et al*[22] showed that miR-29a can decrease the level of inflammatory factors, reduce alveolar epithelial cell apoptosis, and improve lung injury in mice with acute lung injury. Dey *et al*[23] found that miR-29a can inhibit inflammation and fibrosis in acute pancreatitis. Guo *et al*[24] reported that miR-29a can regulate the secretion of luteinizing hormone, thus affecting ovulation in mice. Some studies have shown that miR-29a is present in Exos released by BMSCs and can significantly inhibit the expression of matrix metalloproteinase (MMP)-13 induced by the pro-inflammatory factor interleukin (IL)-6; it can also suppress cartilage degradation and promote cartilage and bone regeneration[25,26]. Although there are fewer reports on miR-29a in studies related to orthopedic disorders, its role in anti-inflammation, promotion of cell proliferation, and inhibition of cell apoptosis has received much attention. Therefore, further research on the application of miR-29a in the field of orthopedics is extremely important.

In this study, we loaded miR-29a into Exos derived from BMSCs (BMSCs-Exos) and developed a novel engineered Exo (BMSCs-miR-29a-Exos). We assessed the effectiveness of the engineered Exo in cartilage repair and OA treatment. The methods commonly used in published studies for engineering Exos include electroporation, transfection, and ultrasound. Among these, ultrasound is easy to operate and has high loading efficiency. Therefore, we used ultrasound to engineer Exos and conducted experiments using a KOA rat model. Through intra-articular injection, the progression of KOA was compared and analyzed among different rat groups from various aspects, such as general behavior, imaging, gross histology, and pathology, to evaluate the effectiveness of BMSCs-miR-29a-Exos in the treatment of KOA. Due to the unique structure of cartilage, we investigated the regulatory effect of BMSCs-miR-29a-Exos on the extracellular matrix of chondrocytes to provide new insights into and options for cartilage repair and regeneration and early-stage OA treatment.

## MATERIALS AND METHODS

### Recovery and culturing of BMSCs

Thawed primary human BMSCs were centrifuged and resuspended in a complete culture medium. Then, they were cultured in an incubator at 37 °C and 5% CO<sub>2</sub> for 72-96 h. After incubation, the culture medium was replaced every three days until the cells reached around 90% confluence. To conduct cell passage, they were briefly treated with trypsin, and the digestion was stopped with a complete culture medium. Finally, cell passage was conducted at a 1:2 ratio for further growth and observation.

### Extraction and identification of BMSCs-Exos

**Extraction of BMSCs-Exos:** The cell culture supernatant was collected in a centrifuge tube and centrifuged for 10 min at 4 °C and 500 × g to remove non-adherent cells and impurities. The resulting supernatant was further centrifuged for 30 min at 4 °C and 2,000 × g, and then, for 60 min at 4 °C and 10000 × g. The supernatant was filtered through a 0.22 μm filter membrane, followed by ultracentrifugation for 70 min at 4 °C and 120000 × g to remove the supernatant. The remaining pellet was resuspended in sterile phosphate buffered saline (PBS) to obtain the BMSCs-Exos suspension.

**Identification of BMSCs-Exos:** Transmission electron microscopy (TEM): BMSCs-Exos solution (10 μL), pre-fixed with 2.5% glutaraldehyde, was dropped onto a copper grid and left at room temperature for 10 min. Excess liquid was removed with filter paper, and then 10 μL of 2% phosphotungstic acid solution (pH = 6.5) was added to the copper grid. After staining for 2 min at room temperature, excess liquid was removed again with filter paper, and the grid was air-dried. TEM was performed to observe and capture images. Nanoparticle tracking analysis (NTA): The BMSCs-Exos were diluted in sterile PBS, filtered through a 0.22 μm filter membrane, and analyzed using a particle size analyzer. Western

blotting (WB) assay: Surface marker proteins of BMSCs-Exos were mixed with a sample buffer, heated in a water bath at 100 °C for 5 min, and then thoroughly centrifuged (20min, 4 °C, 12000 rpm) and placed on ice. A separation gel solution was prepared, and after loading the gel cassette, the separating gel was added. Then, isopropanol was used to seal the top. Once the lower gel solidified, isopropanol was removed, and double-distilled water was used for rinsing. A concentration gel was prepared, and care was taken to avoid bubble formation. A comb was inserted at the appropriate time and removed after gel solidification. The gel cassette was placed on ice, the electrophoresis buffer was poured in, the samples were loaded (about 25 µL per well), and electrophoresis was performed first on the upper gel (60 V, 30 min) and then on the lower gel (110 V, 120 min). Finally, the gels were rinsed with PBS for 2 min. Next, the gel was equilibrated in a transfer buffer. The polyvinylidene fluoride (PVDF) membrane was soaked in methanol (2 min) and double-distilled water (2 min). It was then soaked along with filter paper in the transfer buffer (15 min). The assembly was set up as follows (black plate-fiber pad-filter paper-gel-PVDF membrane-filter paper-fiber pad-white plate) and clamped in a transfer unit (back to back). After filling with the transfer buffer, membrane transfer was performed on ice (100 V and 50 min), followed by soaking in PBS (5 min). The membrane was cut and blocked with 5% skim milk (0.75 g milk powder + 15 mL PBS) (37 °C, 1 h). The blocked membrane was washed thrice with PBS-T (1000 mL 1 × PBS + 1 mL Tween-20) (8 min per wash). The primary antibodies were diluted to 1:2000, and the membrane was incubated overnight in a dish with the primary antibodies at 4 °C on a shaker. The membrane was washed thrice with PBS-T (8 min per wash). Finally, the membrane was placed on a flat surface, developed, and exposed, and the band images were obtained.

### **Preparation and identification of BMSCs-miR-29a-Exos**

**Preparation of BMSCs-miR-29a-Exos:** The miR-29a powder was reconstituted in ddH<sub>2</sub>O to prepare a 100 µmol/L solution. Subsequently, 300 µg of Exos was mixed with 121.6 µL of the aforementioned solution, vortexed, and placed on ice. Ultrasonication was performed at 20% amplitude (on for 30 s and off for 3 min) for six cycles. After ultrasonication, the mixture was incubated at 37 °C for 60 min to restore the Exo membranes. The mixture was then subjected to high-speed centrifugation at 4 °C for 70 min at 120000 × *g*, after which the supernatant was removed. The pellet was resuspended in sterile PBS to obtain the BMSCs-miR-29a-Exo suspension.

**Identification of BMSCs-miR-29a-Exos:** NTA: BMSCs-miR-29a-Exos were diluted in sterile PBS, filtered through a 0.22 µm membrane, and analyzed using a particle size detection instrument. Quantitative reverse transcription polymerase chain reaction (qRT-PCR): RNA extraction: First, 250 µL of Exos was mixed with 750 µL of RNAiso plus and lysed for 5 min. Then, 5 µL of 25 fmol cel-miR-39 external reference was added, followed by the addition of 200 µL of chloroform. After vigorous mixing, the mixture was incubated at room temperature for 5 min and then centrifuged for 15 min at 4 °C at 12000 × *g*. The upper aqueous phase was transferred to another centrifuge tube, and 1/100 volume of Dr. GenTLE Precipitation Carrier (precipitation enhancer) and 1/10 volume of 3 M sodium acetate (pH = 5.2) solution were added and mixed; then, 2.5 times the volume of anhydrous ethanol was added. The mixture was mixed thoroughly and centrifuged for 15 min at 4 °C at 12000 × *g*. The supernatant was discarded, and 1 mL of 70% ethanol (prepared with DEPC water) was added to wash the precipitate. The precipitate was inverted and mixed 6-8 times and centrifuged for 5 min at 4 °C and 8000 × *g*. The supernatant was discarded, and the precipitate was air-dried at room temperature. RNA was dissolved in 20 µL of DEPC H<sub>2</sub>O; DEPC H<sub>2</sub>O was also used as a blank control. Finally, 2 µL of RNA solution was used for analyzing the purity and concentration of RNA *via* spectrophotometry.

Reverse transcription of miRNA: A denaturation solution was prepared following the instructions provided with the kit. An adequate quantity of the above solution was placed in a PCR tube, and RNA was mixed with the denaturation solution for 5 min at 65 °C, followed by rapid cooling on ice. Next, 10 µL of the prepared reverse transcription reaction mixture was added to the PCR tube, mixed, and incubated at 42 °C for 60 min, followed by incubation at 95 °C for 5 min. The reaction mixture was then stored on ice.

Fluorescent quantitative PCR amplification: We prepared a PCR amplification reaction system and performed real-time PCR using a fluorescence quantitative PCR instrument. The PCR cycling consisted of stage 1 (95 °C, 10 min), stage 2 (95 °C, 15 s; 60 °C, 60 s) for 46 cycles, and a dissociation stage to detect the CT value.

### **In vivo animal studies**

**Rat surgical procedure for establishing the OA model:** All animal studies were approved by the Animal Welfare and Ethics Committee of the Affiliated Zhongshan Hospital of Dalian University (No. 2022011010). The rat OA model was established using the Hulth method[27]. Eight-week-old female Sprague Dawley (SD) rats (400-450 g) were continuously anesthetized with 4% isoflurane using a small animal anesthesia machine. Then, the knee was disinfected, and the region above the inner tibia was incised. The patellar ligament was exposed and incised, following which, the joint capsule was opened. The anterior cruciate ligament was cut and confirmed with an anterior drawer test. Then, the partial medial meniscus was removed, and hemostasis, joint cavity irrigation, and layered closure were performed. The date of the surgery was recorded. Animals assigned to experimental groups were managed following husbandry protocols. The 36 rats were divided into three groups (*n* = 6), which included the EXO group, the E-Exo group, and the NC group (without any scaffold).

**Knee joint cavity injection in rats:** The rats were anesthetized with isoflurane, and the knee joint space was identified and marked. The area was disinfected following standard disinfection procedures. Using a 1 mL syringe, 100 µL of a specific liquid was injected into the joint space on the medial side of the patellar ligament, depending on the groups that the rats were assigned to. In the NC group, the liquid injected was physiological saline; in the Exo group, it was a suspension of BMSCs-Exos (10<sup>9</sup>/mL); in the E-Exo group, the liquid injected was a suspension of BMSCs-miR-29a-Exos

(10°/mL). The liquid was injected into the right knee joint space of the rats, with slow injection after confirming no occurrence of blood backflow. The syringe was held steady after injection, and the knee joint was gently moved to ensure even distribution of the liquid. The needle was slowly withdrawn to prevent leakage of the liquid. The rats were sacrificed four weeks and eight weeks after surgery. The whole cranium plus scaffold was harvested and fixed in 4% paraformaldehyde for histological analysis.

**General behavioral observations in rats:** The general behavioral performance of the rats was recorded postoperatively and graded according to the Lequesne MG criteria[28] for comparing the behavioral performance of the rats.

**Micro-computed tomography scans:** After the rats were sacrificed by the cervical dislocation method, the right lower limb was intercepted and the soft tissues around the joint were removed as much as possible while keeping the knee joint intact. The tissues were sterilized and placed on a carbon fiber specimen plate of the micro-computed tomography (CT) machine, fixed firmly with tape. Scanning was performed according to the operating procedure.

**Gross observation of articular cartilage:** The joint surface of the right knee joint of the rats was exposed, observed, compared among the groups, and photographed. The joint surfaces of the rats were scored according to the Pelletier gross scoring criteria[24] (Table 1).

**Histology and immunohistochemistry:** All samples were decalcified in 15% ethylenediaminetetraacetic acid (pH = 7.2) and refreshed every three days for four weeks. After the samples were dehydrated using a tissue processor, they were embedded in paraffin, and cut into serial 4- $\mu$ m sections (Leica, Germany) for staining. The pathological sections of each group were evaluated by hematoxylin and eosin staining (H&E; Solarbio, China) and Red O-solid green (Solarbio, China) staining. All images were captured using a light optical microscope (Olympus, Japan).

The tissues were blocked and sealed by washing them with PBS thrice (5 min per wash), marking them with an immunohistochemistry pen, blocking with 3% hydrogen peroxide for 18 min, washing again with PBS for 5 min, and sealing with goat serum for 15 min. The tissues were incubated with primary antibodies (1:300 dilution) overnight at 4 °C. After incubation, the tissues were washed with PBS for 5 min and brought to room temperature (5 min). These tissues were labeled with secondary antibodies for 15 min at room temperature and then washed again with PBS for 5 min. DAB staining was performed by evenly applying a light-protected DAB solution to the tissues, incubating for 5 min at room temperature, monitoring color changes, and terminating the reaction with distilled water. Next, the samples were stained with hematoxylin for 30 s and rinsed thrice with distilled water (5 min per wash). The tissues were dehydrated and cleaned in graded ethanol and xylene (3 min per step in 75%, 85%, 95% ethanol, and two xylene steps). Finally, the tissues were mounted in neutral resin and observed under a microscope.

### Statistical analysis

Statistical analysis was performed using the SPSS 23.0 software. The differences between any two groups were evaluated by *t*-tests, and the differences among multiple groups were evaluated by a one-way analysis of variance (ANOVA). All differences among and between groups were considered to be statistically significant at  $P < 0.05$ ;  $P < 0.01$  indicated a significant difference,  $P < 0.001$  indicated a highly significant difference, and  $P > 0.05$  indicated that the differences were not statistically significant.

## RESULTS

### Extraction and identification of BMSCs-Exos

By day 7, almost all BMSCs were spindle-shaped. When the cells grew to 80% confluence, Exos were extracted (Figure 1A). The Exos were observed *via* TEM; they had a circular appearance. The appearance and diameter were consistent with Exos reported in other studies (Figure 1B). The Exos samples were diluted eight times with PBS and then injected into the sample for detection. The NTA results showed that the concentration of BMSC-Exos was  $3.43 \times 10^9$ /mL, with a mean particle size of 131.9 nm and a concentrated distribution (Figure 1C). The results of the WB assay of Exos surface markers showed a positive expression of CD9, heat shock protein 70, and tumor necrosis factor- $\alpha$ -stimulated gene 101 (Figure 1D). These results confirmed that they were BMSCs-Exos.

### Identification of BMSCs-miR-29a-Exos

**NTA:** After the BMSCs-miR-29a-Exos were prepared by ultrasonication, the BMSCs-miR-29a-Exos samples were diluted 2.3 times with PBS and the results of NTA detection showed that the concentration of the obtained BMSCs-miR-29a-Exos was  $1.62 \times 10^9$ /mL, the average particle size was 173.7 nm, and the particles were concentrated (Figure 2). The mean particle size of BMSCs-miR-29a-Exos was significantly greater than that of BMSCs-Exos.

**qRT-PCR:** The results of the qRT-PCR assay showed that the expression of miR-29a was significantly upregulated in BMSCs-miR-29a-Exos compared to its expression in BMSCs-Exos (Figure 3).

### Assessment of the ability of BMSCs-miR-29a-Exos injected in the knee to delay the progression of OA

**Postoperative rat survival rate and general behavioral observations:** All 36 rats in the three groups recovered after surgery. The incision healed adequately, and no mortal injuries or infections from other diseases were recorded. The

**Table 1** The Pelletier gross scoring criteria

Articular surface conditions	Rating
The articular surfaces are intact and of normal color	0
The articular surface is slightly rough, with small fissures visible and loss of luster	1
Mild damage to the articular surface, with cartilage damage reaching the superficial or middle cartilage layer	2
The articular surface is heavily damaged, with the defect reaching deep into the cartilage but not yet exposing the subchondral bone	3
The cartilage defect is severe, and the subchondral bone is exposed or even damaged	4

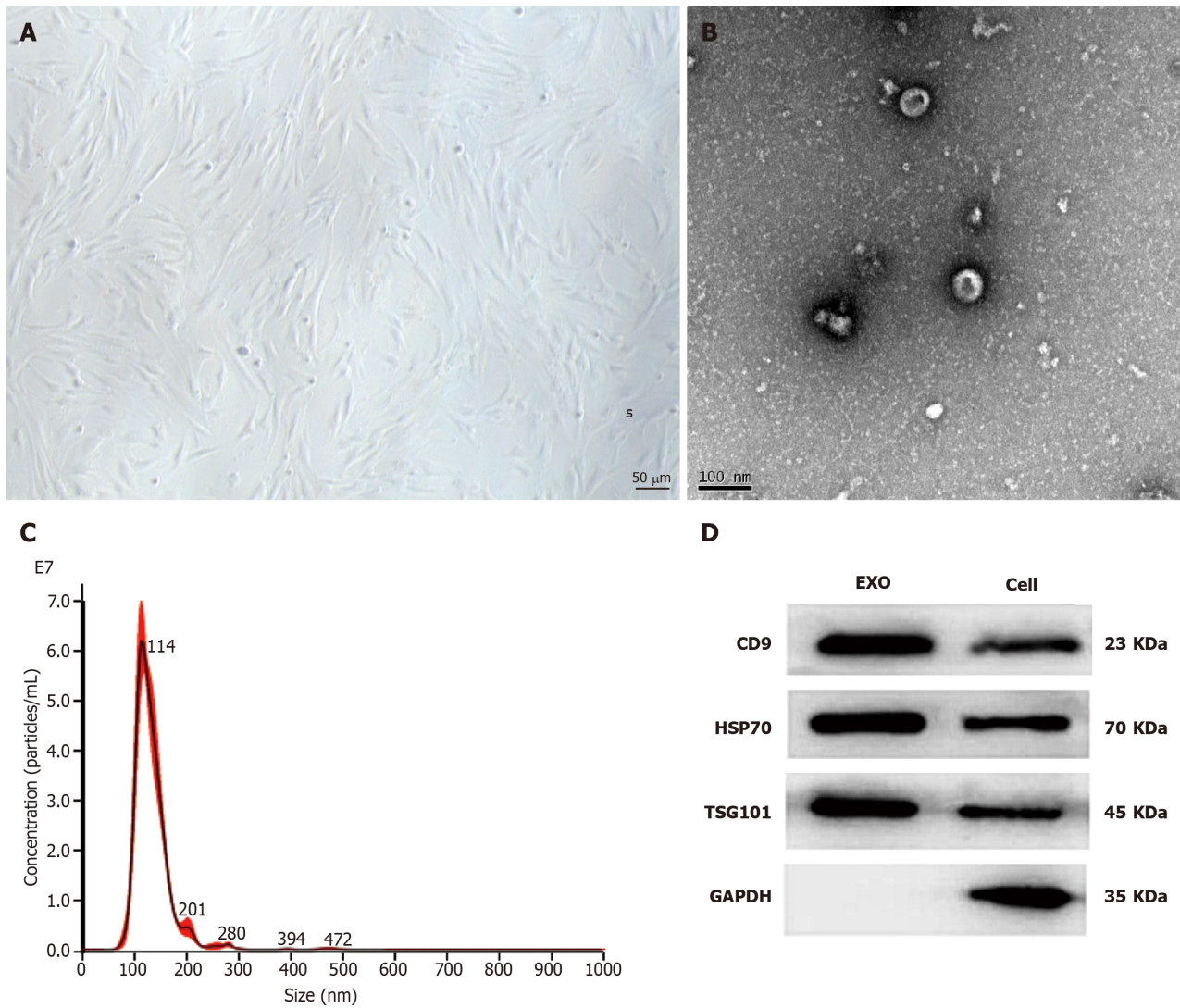


**Figure 1** Morphological observation of bone marrow-derived mesenchymal stem cells and identification of bone marrow-derived mesenchymal stem cells-exosomes. A: The bone marrow-derived mesenchymal stem cells (BMSCs) had a homogeneous spindle morphology; B: The BMSC-exosomes (Exos) were approximately 60–160 nm in diameter and had a sub-circular, typical teatoid appearance; C: The nanoparticle tracking analysis results showed that the concentration of BMSC-Exos was  $3.43 \times 10^9/\text{mL}$  and their average particle size was 131.9 nm; D: The results of the western blotting assays showed that the expression of CD9, heat shock protein 70, and tumor necrosis factor- $\alpha$ -stimulated gene 101 was positive. Exo: Exosomes; HSP: Heat shock protein; TSG: Tumor necrosis factor- $\alpha$ -stimulated gene.

Lequesne MG grading was used to compare pain, gait condition, knee range of motion, and swelling at two time points (Table 2). The results showed that rats in the Exo and E-Exo groups had lesser OA than those in the NC group. At four weeks, the rats in the E-Exo group had lesser pain than those in the Exo group. At eight weeks, the rats in the E-Exo group had better knee range of motion than those in the Exo group (Table 3). The differences in the other parameters between these two groups were not statistically significant.

**Micro-CT of the rat knee joint:** Four weeks: Most specimens in the NC group showed bone redundancy, damage to the

Table 2 The Lequesne MG rating criteria

	Level 1	Level 2	Level 3	Level 4
Pain conditions	No significant reaction	Avoidance contraction of the affected limb following compression	Avoided contraction of the affected limb and turn back, body out present tremor	Violent contraction of the affected limb, violent shaking and struggling of the body
Gait	Normal gait	Mild limp but strong stirring of the affected limb	The limp is pronounced, and the strength of the affected limb to stir on the ground is reduced	The affected limb is afraid to walk on the ground
Knee range of motion	> 90°	45°-90°	15°-45°	< 15°
Swelling	No swelling and clear bony markings	Mild swelling with superficial bony markings	Significant swelling and loss of bony markings	

articular surface, and subchondral bone fractures. Some specimens in the Exo group showed a small amount of bone redundancy, uneven articular surface, and sclerotic band formation. However, no significant bone redundancy was recorded in the E-Exo group, and no significant damage to the articular surface was found in this group. Eight weeks: Most specimens in the NC group had severe joint damage and a significantly reduced joint space. The samples in the Exo group showed more damage to the joint surface and reduced joint space. The samples in the E-Exo group had visible bone formation, visible joint surface damage, sclerotic band formation, and fair joint space (Figure 4).

**Gross observation of the knee joint in rats:** Four weeks: The samples in the NC group had slightly uneven articular surfaces, as seen by the naked eye. Scattered hemorrhages were found on the articular surfaces, and the cartilage surfaces were worn. The samples in the Exo group did not show any signs of hemorrhage; slight synovial hyperplasia was found, and some specimens had slightly uneven cartilage surfaces. The samples in the E-Exo group did not show any signs of OA. Eight weeks: Yellowish and viscous joint fluid was found in the samples of the NC group; these samples also showed marked synovial hyperplasia, considerable wear and tear, or even breakdown of the cartilage surface, and loss of luster on the articular surface. The samples in the Exo group showed slightly turbid joint fluid, mild synovial hyperplasia, uneven articular cartilage surface, slight wear and tear on some cartilage surfaces, and uneven articular surface. The samples in the E-Exo group showed a clear and transparent joint fluid, mild synovial hyperplasia (visible in some specimens), and no marked wear and tear on the articular cartilage surface. No significant wear was found on the articular cartilage surfaces (Figure 5).

The results of Pelletier's gross scores showed that at four weeks, the scores of the NC group were greater than those of the Exo and E-Exo groups; the scores of the Exo and E-Exo groups were not significantly different. At eight weeks, the scores of the NC group were significantly greater than those of the Exo and E-Exo groups ( $P < 0.05$ ); also, the scores of the Exo group were significantly greater than those of the E-Exo group ( $P < 0.05$ ) (Figure 6A).

**Histological staining analysis:** H&E staining: At four weeks, the cartilage surface of all groups was smooth, the cartilage layer of the NC group was thin, the cartilage surface was flat, the cartilage matrix staining was light, and the samples showed prominent degeneration. The cartilage layer of the Exo group was thicker than NC group, and the number of chondrocytes was slightly lower. The cartilage layer of the E-Exo group was thicker than that of the other two groups, and the number of cells was higher. At eight weeks, the cartilage layer of the NC group was severely eroded, the number of chondrocytes was substantially lower, and the joint surface was severely damaged. The cartilage layer was thicker in the E-Exo group than in the Exo group; the chondrocytes were still neatly arranged, and the number of cells was higher in the E-Exo group than in the Exo group (Figure 7A).

Fuchsin O-solid green staining: At four weeks, cartilage staining in the NC group was reduced, sclerotic bone was formed on the cartilage surface, and the articular cartilage surface was uneven. In the Exo group, cartilage staining was slightly reduced, and the articular surface was still flat. The cartilage layer was significantly thicker in the E-Exo group than in the other two groups; the staining was uniform, and the cells were well-arranged in the E-Exo group. At eight weeks, cartilage staining in the NC group was severely reduced, some cartilage cells were clustered, and the articular cartilage surface was severely damaged. In the Exo group, cartilage staining was reduced, and the articular cartilage surface was damaged. In the E-Exo group, cartilage staining was more uniform, and the articular cartilage surface was still flat (Figure 7B).

The results of the modified Mankin score showed that at four weeks, the score of the NC group was greater than that of the Exo and E-Exo groups; however, no significant difference between the scores of the Exo and E-Exo groups was recorded. At eight weeks, the score of the NC group was significantly higher than that of the Exo and E-Exo groups ( $P < 0.05$ ), and the score of the Exo group was significantly higher than that of the E-Exo group ( $P < 0.05$ ) (Figure 6B).

**Immunohistochemical staining analysis:** Type II collagen expression: At four weeks, the NC group showed less positive expression of type II collagen in the cytoplasm of chondrocytes. Only some chondrocytes showed a positive expression and a lighter yellow color. The Exo group showed more positive expression with a darker yellow color than the NC group. The E-Exo group showed positive expression (yellow color) in the cytoplasm of a large number of chondrocytes, and the color was darker in this group than that recorded in the other two groups; this indicated that the expression of

Table 3 Comparison of Lequesne MG grades at three different time points

Group	Localized pain assessment				Gait assessment				Knee joint range of motion assessment				Swelling condition assessment		
	Level 1	Level 2	Level 3	Level 4	Level 1	Level 2	Level 3	Level 4	Level 1	Level 2	Level 3	Level 4	Level 1	Level 2	Level 3
4-wk NC group	2	6	4	0	1	7	4	0	0	8	3	1	0	8	4
4-wk Exo group	8	3	1	0	3	8	1	0	6	5	1	0	9	3	0
4-wk E-Exo group	11	1	0	0	4	6	2	0	7	5	0	0	10	2	0
8-wk NC group	0	1	3	2	0	2	3	1	0	1	3	2	0	2	4
8-wk Exo group	3	2	1	0	2	3	1	0	0	4	2	0	3	3	0
8-wk E-Exo group	4	2	0	0	1	4	1	0	2	3	1	0	4	2	0

Exo: Exosomes; NC: Negative control.

collagen was the strongest in the E-Exo group. In the Exo group, the articular surface was not smooth, and some chondrocytes were clustered; positive expression was found in the cytoplasm, which was lighter in color. In the E-Exo group, the articular surface was poor, and the chondrocytes were more evenly distributed, although a few chondrocytes were clustered. A more positive and stronger expression was recorded in the E-Exo group than in the other two groups (Figure 8A).

Proteoglycan expression: At four weeks, the NC group had a less positive expression of proteoglycans in the cytoplasm of chondrocytes. Only a few chondrocytes were positive, and they had a very light yellow color. The Exo group showed more positive expression and a darker yellow color than the NC group. The E-Exo group showed a prominent yellow color, indicating a positive expression of proteoglycans in the cytoplasm of many chondrocytes; the color was darker than that observed in the other two groups, which indicated that the expression of proteoglycans was the strongest in the E-Exo group. In the E-Exo group, the articular cartilage surface was not well-developed, and the chondrocytes were more evenly distributed, although a few chondrocytes were found in clusters (Figure 8B).

## DISCUSSION

OA is a complex disease caused by various factors, which results in joint pain, restricted movement, and swelling[1,29]. The prevalence of OA is high, and with the general trend of increase in life expectancy and body mass index, the incidence of OA is increasing year-on-year; KOA is responsible for more than 80% of the total cases of OA[30]. Due to the special structure of articular cartilage, its blood supply is insufficient, which makes self-repair of damaged cartilage difficult. Therefore, an effective method is required to repair cartilage. Depending on the situation and requirements of the patient, KOA treatment is divided into surgical and non-surgical treatments. Arthroplasty is the best option for patients with end-stage KOA, which can relieve pain and correct deformity at the source, but the function of the joint and the life of the prosthesis are uncertain after arthroplasty[31]. Current treatment for patients with early KOA is mostly

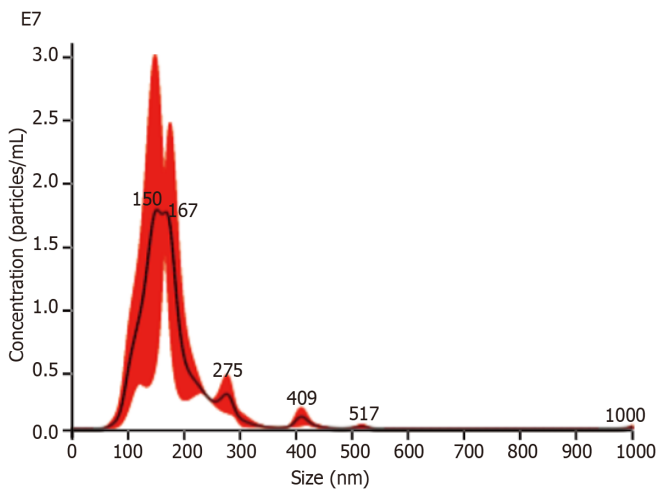


**Figure 2** The results of nanoparticle tracking analysis of bone marrow-derived mesenchymal stem cells-miR-29a-Exos.

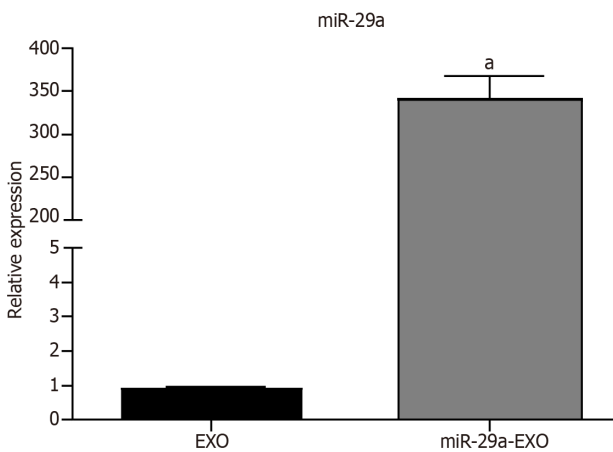
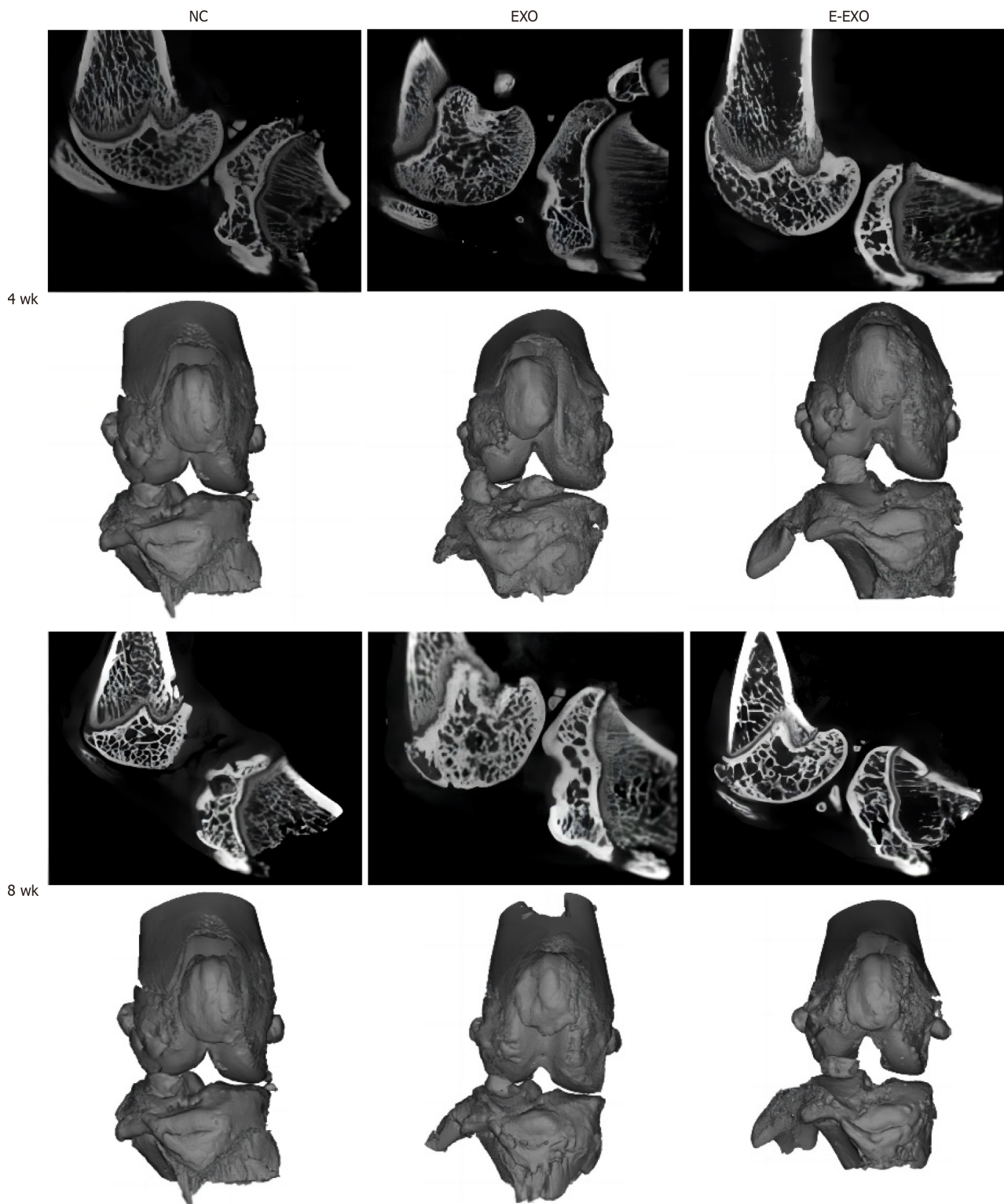


**Figure 3** The results of the quantitative reverse transcription polymerase chain reaction assay, <sup>a</sup>*P* < 0.001. Exo: Exosomes.

non-curative and symptomatic. No known drugs approved for regulatory use can substantially improve KOA[32]. Therefore, in this study, we investigated a drug that can be used to treat KOA through knee injections to provide a new strategy for the treatment of cartilage injury and OA.

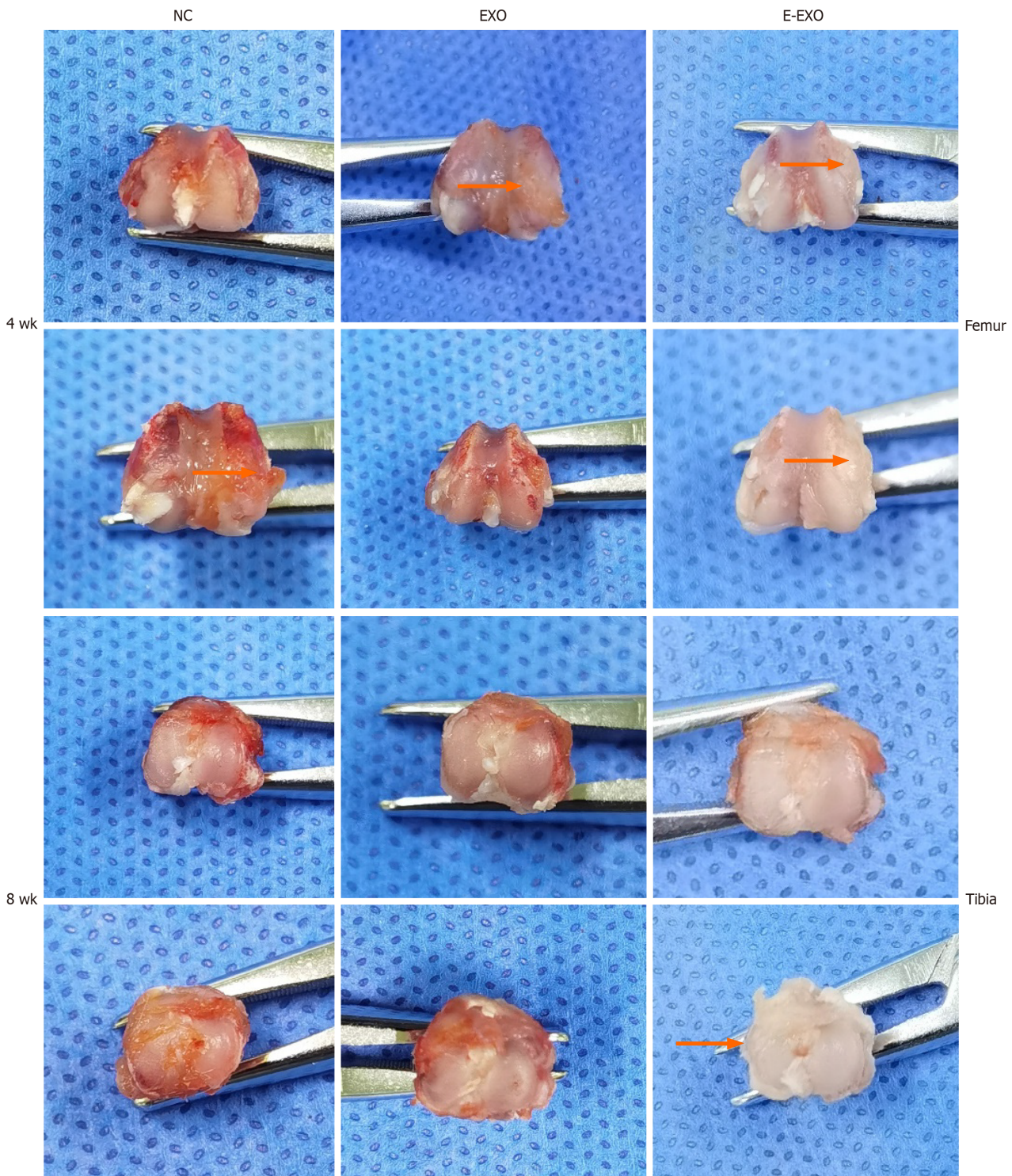
Animal models are often used to test the effectiveness of interventions before clinical trials are conducted; the selection of an appropriate animal model is crucial to the effectiveness of the study. Knee KOA can be modeled in various ways [33]. First, we calculated the number of animals required according to the number of treatment groups needed in the study and assessed the cost, feeding period, resistance to infection, and cartilage condition of the commonly used animals. Based on our criteria, SD rats were the most suitable to build the model. After an extensive literature survey, we found that there are many methods to construct the KOA rat model, including the anterior cruciate ligament dissection method[34], the anterior cruciate ligament dissection + partial medial meniscectomy method[35,36], the medial collateral ligament dissection + medial meniscectomy method[37], and the mono-iodoacetic acid joint injection method[38]. In this study, we stimulated the development of KOA and investigated whether BMSCs-miR-29a-Exos intra-articular injection can modulate the extracellular matrix to delay the progression of KOA. The modeling period of anterior cruciate dissection + partial medial meniscectomy was found to be more compatible with the design of this study and could better simulate the development of KOA. Hence, the method involving anterior cruciate dissection + partial medial meniscectomy was selected to establish the rat KOA model. During the pre-experimental and experimental phases, the rats in the NC group showed pain and uneasy movement of the knee joint after modeling, and the symptoms worsened over time.

Many researchers have investigated the treatment of KOA using treatment methods involving BMSCs. Many studies have found that BMSCs are promising for the treatment of KOA, as they can be stimulated to differentiate into cartilage and repair cartilage tissue. They can also inhibit the inflammatory response during the development of KOA, and thus, they can facilitate the treatment of KOA in multiple ways[39,40]. Some researchers used BMSCs in the clinical treatment of traumatic articular cartilage defects and reported relatively positive results[41]. The discovery and study of BMSCs-Exos has provided new opportunities for researchers to explore the treatment of KOA. As BMSCs-Exos can regulate the extracellular matrix, they might be able to repair cartilage and treat KOA[42]. Following extensive research on BMSCs, researchers have also obtained valuable results by studying Exos; several studies have found that the proteins, lipids, and



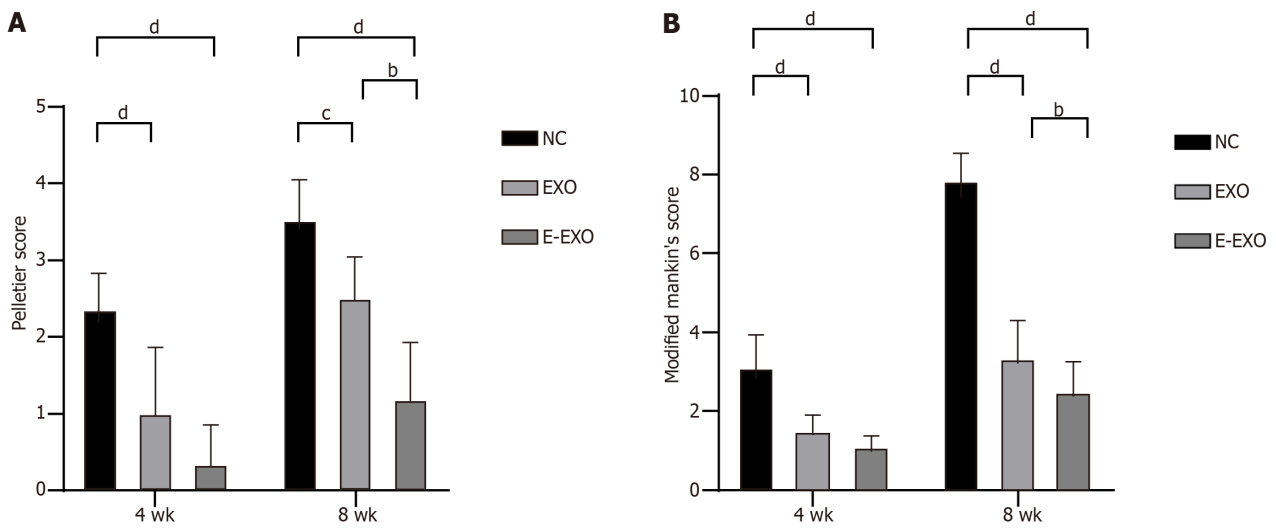
**Figure 4** Micro-computed tomography and three-dimensional reconstruction of the knee joint of rats. Micro-computed tomography images of the knee joint and the 3D reconstructed images of the corresponding specimens for each group of rats at four weeks and eight weeks are presented. Exo: Exosomes; NC: Negative control.

nucleic acids associated with Exos have important functions[43]. For example, miR-29a in BMSCs-Exos can significantly inhibit the expression of MMP-13 induced by the pro-inflammatory factor IL-6; through this change, they can inhibit the degeneration of articular cartilage and promote the regeneration of articular cartilage and bone[25,26]. Researchers needed natural Exos to carry larger quantities of relevant functional small molecules; thus, they modified natural Exos using various modalities. Some researchers developed E-Exos, following which research on E-Exos progressed rapidly with some promising results. Due to the effectiveness of E-Exos, our group conducted this study. We first prepared BMSCs-miR-29a-Exos using ultrasound. Then, we designed animal experiments to establish a rat KOA model and investigated the effect of knee injection of BMSCs-miR-29a-Exos on the progression of KOA in a rat model of KOA. We set up a



**Figure 5** Photographs of gross specimens of rat knee joints. Exo: Exosomes; NC: Negative control.

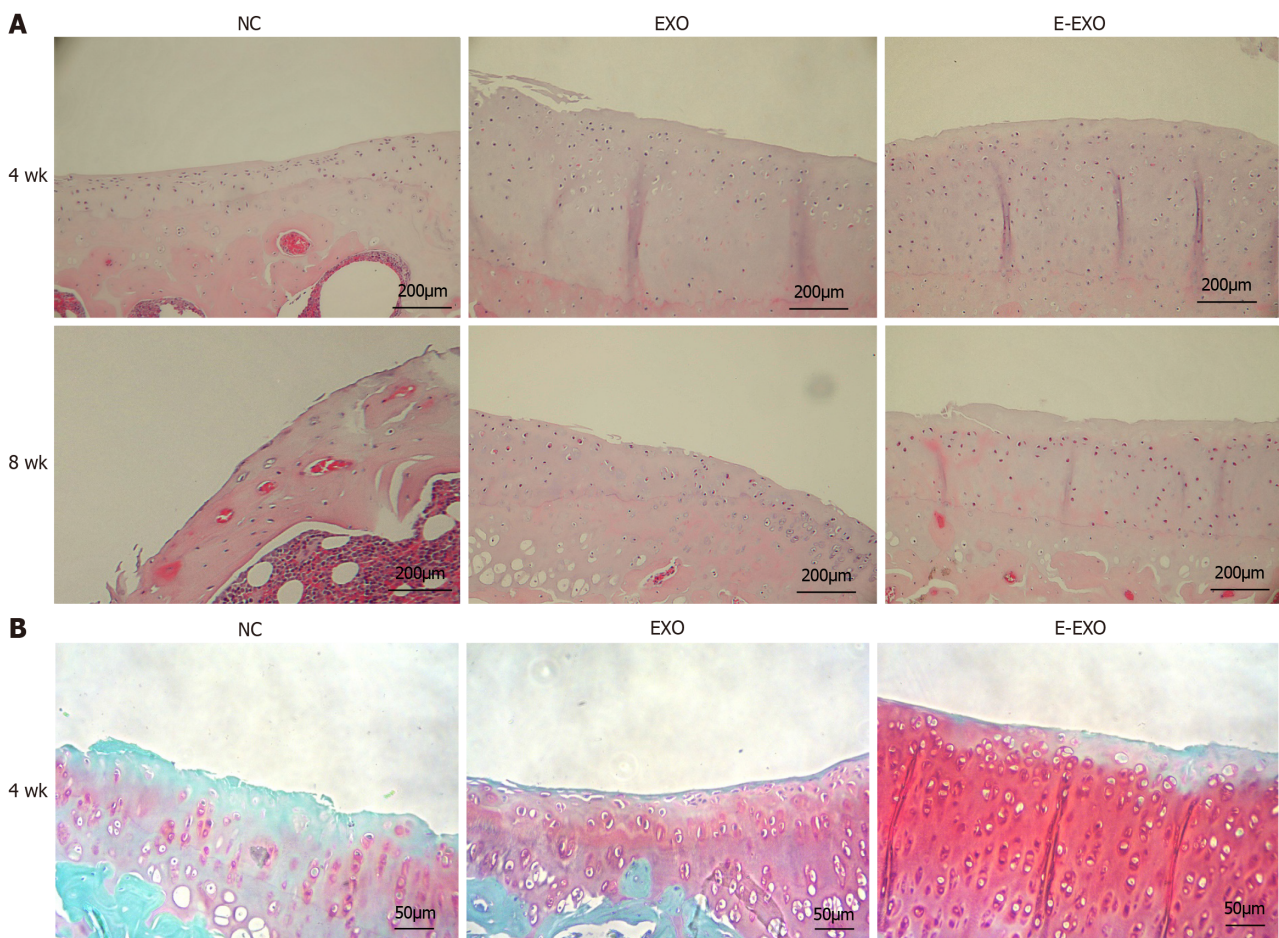
suitable control group to compare it with the BMSCs-Exos and saline groups. We found that after injecting BMSCs-Exos/BMSCs-miR-29a-Exos in the knees, the progression of KOA was slower in the above two groups of rats compared to KOA progression in the NC group. The effect of BMSCs-miR-29a-Exos was greater than that of BMSCs-Exos. The results of the general behavioral tests, imaging examinations, gross histological observations, and pathological staining showed that both BMSCs-Exos and BMSCs-miR-29a-Exos delayed the progression of KOA in rats, with BMSCs-miR-29a-Exos being more effective. Immunohistochemical staining results showed that BMSCs-Exos and BMSCs-miR-29a-Exos upregulated the expression of type II collagen and proteoglycans in rat knee joints, and the effect of BMSCs-miR-29a-Exos was more significant, which indicated that BMSCs-Exos and BMSCs-miR-29a-Exos improved the condition of the extracellular matrix of cartilage. The effect of BMSCs-miR-29a-Exos was more significant than that of BMSCs-Exos, which matched our pre-experimental hypothesis.



**Figure 6 Pelletier gross scores and the modified Mankin's score.** A: Pelletier gross scores; B: The modified Mankin's score. <sup>b</sup> $P < 0.01$ , <sup>c</sup> $P < 0.05$ , <sup>d</sup> $P < 0.01$ . Exo: Exosomes; NC: Negative control.

## CONCLUSION

In this study, we found that BMSCs-miR-29a-Exos protected articular cartilage by regulating the extracellular matrix of the cartilage, effectively reducing articular cartilage damage in KOA rats and delaying the progression of KOA. However, we did not further investigate the molecular mechanisms of the upstream signaling molecules. Therefore, we aim to investigate the molecular mechanisms of the upstream signaling molecules in subsequent studies and also use blood and joint tissues to test the relevant inflammatory indices in the future to evaluate their effect on inflammation and elucidate the relevant mechanisms.



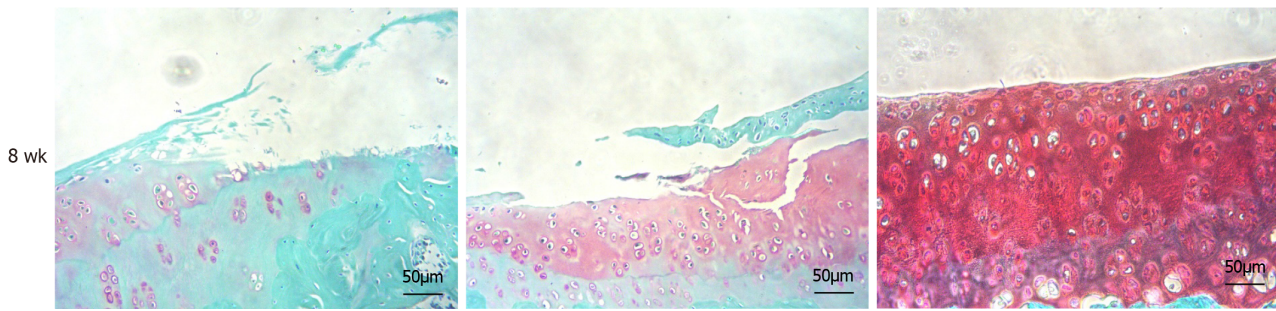


**Figure 7** Images of the condyles of femur of rats stained with hematoxylin and eosin and Safranin O-fast green. A: Images of the condyles of femur of rats stained with hematoxylin and eosin. We have re-uploaded the images; all of them depict cross-sectional staining of the femoral condyle; B: Images of condyles of femur of rats stained with Safranin O-fast green. Exo: Exosomes; NC: Negative control.

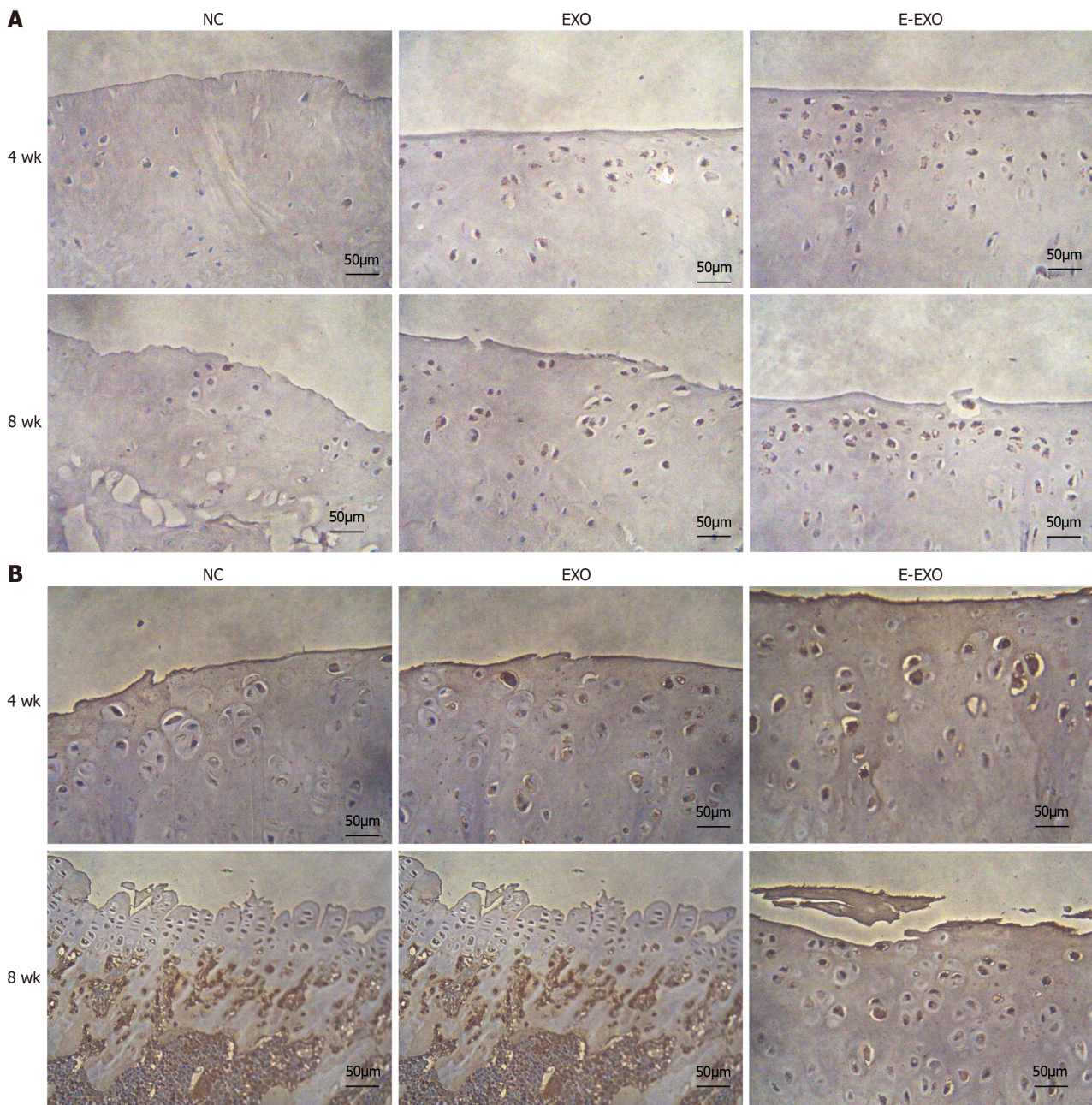


**Figure 8** The expression of type II collagen and proteoglycans. A: The expression of type II collagen; B: The expression of proteoglycans. Exo: Exosomes; NC: Negative control.

## ARTICLE HIGHLIGHTS

### Research background

The main focus is understanding knee osteoarthritis (KOA), exploring genetic and biomechanical factors, and investigating the potential of mesenchymal stem cell (MSC)-derived extracellular vesicles (exosomes) containing miR-29a for early treatment. Key issues include validating safety and efficacy, with resolving these challenges holding significance for advancing effective KOA progression management and future research in the field.

### Research motivation

The primary goal of the study is to investigate miR-29a's role in KOA by creating miR-29a-loaded vesicles and testing their impact in rat models. Achieving this aims to provide insights into early-stage KOA treatment and highlights the potential of extracellular vesicles for future therapeutic interventions in KOA. The significance lies in advancing our understanding of miRNA-based interventions, particularly miR-29a, and paving the way for innovative strategies in the management of KOA progression.

### Research objectives

The study involved extracting extracellular vesicles from bone marrow MSCs, engineering vesicles loaded with miR-29a using ultrasonication, and confirming their content through quantitative reverse transcription polymerase chain reaction. In a rat model of KOA, three groups were established and assessed through various analyses, such as behavioral observation, imaging, histological observation, and immunohistochemical detection, offering a comprehensive approach to evaluating arthritis progression. The unique aspect lies in the application of engineered extracellular vesicles for targeted miR-29a delivery in the context of OA treatment.

### Research methods

The article explores the multifactorial etiology of KOA, emphasizing the potential of MSC-released extracellular vesicles (exosomes) and microRNAs for cartilage regeneration, signaling a promising avenue for future KOA treatment pending further validation.

### Research results

General behavioral observation results showed that the extracellular vesicle group and engineered extracellular vesicle group had better performance in all four indicators of pain, gait, joint mobility, and swelling compared to the blank control group. Imaging examination results showed that the blank control group had the fastest progression of arthritis, the normal extracellular vesicle group had a relatively slower progression, and the engineered extracellular vesicle group had the slowest progression. Gross histological observation results showed that the blank control group had the most obvious signs of arthritis, the normal extracellular vesicle group showed signs of arthritis, and the engineered extracellular vesicle group showed no significant signs of arthritis.

### Research conclusions

The engineered exosomes loaded with miR-29a attenuate the progression of KOA.

### Research perspectives

In future studies, we plan to explore the molecular mechanisms of upstream signaling molecules. We aim to use blood and joint tissue assays to detect inflammation markers, evaluating their influence and elucidating associated mechanisms.

## ACKNOWLEDGEMENTS

The authors would like to thank the members of the Orthopaedic and Cell Analysis Laboratory of Zhongshan Hospital Affiliated to Dalian University and the technical support of the Orthopaedic Laboratory. The author also thanks Professor Liu Bao-Yi for his meticulous language help.

## FOOTNOTES

**Author contributions:** Liu BY and Zhao DW was the guarantor and designed the study; Yang F and Xiong WQ participated in the acquisition, analysis, and interpretation of the data, and drafted the initial manuscript; Li CZ, Wu MJ, Zhang XZ, Ran CX, Li ZH, and Cui Y revised the article critically for important intellectual content.

**Supported by** Project of the National Natural Science Foundation of China, No. 82172398; Key Research Project of the Department of Education of Liaoning Province, No. LJKZZ20220148; Dalian Medical Science Research Project, No. 2111038; and Dalian Dengfeng Plan Medical Key Specialty Construction Project (2021), No. 243.

**Institutional animal care and use committee statement:** All animal studies were approved by the Animal Welfare and Ethics Committee

of the Affiliated Zhongshan Hospital of Dalian University (No. 2022011010).

**Conflict-of-interest statement:** All the authors report no relevant conflicts of interest for this article.

**Data sharing statement:** No additional data are available.

**ARRIVE guidelines statement:** The authors have read the ARRIVE guidelines, and the manuscript was prepared and revised according to the ARRIVE guidelines.

**Open-Access:** This article is an open-access article that was selected by an in-house editor and fully peer-reviewed by external reviewers. It is distributed in accordance with the Creative Commons Attribution NonCommercial (CC BY-NC 4.0) license, which permits others to distribute, remix, adapt, build upon this work non-commercially, and license their derivative works on different terms, provided the original work is properly cited and the use is non-commercial. See: <https://creativecommons.org/licenses/by-nc/4.0/>

**Country/Territory of origin:** China

**ORCID number:** Bao-Yi Liu 0000-0003-3531-415X; De-Wei Zhao 0000-0001-8611-0558.

**S-Editor:** Wang JJ

**L-Editor:** A

**P-Editor:** Zhao YQ

## REFERENCES

- Hunter DJ, Bierma-Zeinstra S. Osteoarthritis. *Lancet* 2019; **393**: 1745-1759 [PMID: 31034380 DOI: 10.1016/S0140-6736(19)30417-9]
- Prieto-Alhambra D, Judge A, Javaid MK, Cooper C, Diez-Perez A, Arden NK. Incidence and risk factors for clinically diagnosed knee, hip and hand osteoarthritis: influences of age, gender and osteoarthritis affecting other joints. *Ann Rheum Dis* 2014; **73**: 1659-1664 [PMID: 23744977 DOI: 10.1136/annrheumdis-2013-203355]
- Kulkarni P, Martson A, Vidya R, Chitnavis S, Harsulkar A. Pathophysiological landscape of osteoarthritis. *Adv Clin Chem* 2021; **100**: 37-90 [PMID: 33453867 DOI: 10.1016/bs.acc.2020.04.002]
- Stanton H, Rogerson FM, East CJ, Golub SB, Lawlor KE, Meeker CT, Little CB, Last K, Farmer PJ, Campbell IK, Fourie AM, Fosang AJ. ADAMTS5 is the major aggrecanase in mouse cartilage *in vivo* and *in vitro*. *Nature* 2005; **434**: 648-652 [PMID: 15800625 DOI: 10.1038/nature03417]
- Amor C, Feucht J, Leibold J, Ho YJ, Zhu C, Alonso-Curbelo D, Mansilla-Soto J, Boyer JA, Li X, Giavridis T, Kulick A, Houlihan S, Peerschke E, Friedman SL, Ponomarev V, Piersigilli A, Sadelain M, Lowe SW. Senolytic CAR T cells reverse senescence-associated pathologies. *Nature* 2020; **583**: 127-132 [PMID: 32555459 DOI: 10.1038/s41586-020-2403-9]
- Lakin BA, Snyder BD, Grinstaff MW. Assessing Cartilage Biomechanical Properties: Techniques for Evaluating the Functional Performance of Cartilage in Health and Disease. *Annu Rev Biomed Eng* 2017; **19**: 27-55 [PMID: 28226218 DOI: 10.1146/annurev-bioeng-071516-044525]
- Kong H, Wang XQ, Zhang XA. Exercise for Osteoarthritis: A Literature Review of Pathology and Mechanism. *Front Aging Neurosci* 2022; **14**: 854026 [PMID: 35592699 DOI: 10.3389/fnagi.2022.854026]
- Glyn-Jones S, Palmer AJ, Agricola R, Price AJ, Vincent TL, Weinans H, Carr AJ. Osteoarthritis. *Lancet* 2015; **386**: 376-387 [PMID: 25748615 DOI: 10.1016/S0140-6736(14)60802-3]
- Bierma-Zeinstra S, van Middelkoop M, Runhaar J, Schiphof D. Nonpharmacological and nonsurgical approaches in OA. *Best Pract Res Clin Rheumatol* 2020; **34**: 101564 [PMID: 32773214 DOI: 10.1016/j.berh.2020.101564]
- McAlindon TE, Bannuru RR, Sullivan MC, Arden NK, Berenbaum F, Bierma-Zeinstra SM, Hawker GA, Henrotin Y, Hunter DJ, Kawaguchi H, Kwok K, Lohmander S, Rannou F, Roos EM, Underwood M. OARSJ guidelines for the non-surgical management of knee osteoarthritis. *Osteoarthritis Cartilage* 2014; **22**: 363-388 [PMID: 24462672 DOI: 10.1016/j.joca.2014.01.003]
- Latourte A, Kloppenburg M, Richette P. Emerging pharmaceutical therapies for osteoarthritis. *Nat Rev Rheumatol* 2020; **16**: 673-688 [PMID: 33122845 DOI: 10.1038/s41584-020-00518-6]
- Maumus M, Jorgensen C, Noël D. Mesenchymal stem cells in regenerative medicine applied to rheumatic diseases: role of secretome and exosomes. *Biochimie* 2013; **95**: 2229-2234 [PMID: 23685070 DOI: 10.1016/j.biochi.2013.04.017]
- Pers YM, Ruiz M, Noël D, Jorgensen C. Mesenchymal stem cells for the management of inflammation in osteoarthritis: state of the art and perspectives. *Osteoarthritis Cartilage* 2015; **23**: 2027-2035 [PMID: 26521749 DOI: 10.1016/j.joca.2015.07.004]
- Chu DT, Phuong TNT, Tien NLB, Tran DK, Thanh VV, Quang TL, Truong DT, Pham VH, Ngoc VTN, Chu-Dinh T, Kushekhar K. An Update on the Progress of Isolation, Culture, Storage, and Clinical Application of Human Bone Marrow Mesenchymal Stem/Stromal Cells. *Int J Mol Sci* 2020; **21** [PMID: 31973182 DOI: 10.3390/ijms21030708]
- Bao C, He C. The role and therapeutic potential of MSC-derived exosomes in osteoarthritis. *Arch Biochem Biophys* 2021; **710**: 109002 [PMID: 34352243 DOI: 10.1016/j.abb.2021.109002]
- Kwon DG, Kim MK, Jeon YS, Nam YC, Park JS, Ryu DJ. State of the Art: The Immunomodulatory Role of MSCs for Osteoarthritis. *Int J Mol Sci* 2022; **23** [PMID: 35163541 DOI: 10.3390/ijms23031618]
- Wu J, Kuang L, Chen C, Yang J, Zeng WN, Li T, Chen H, Huang S, Fu Z, Li J, Liu R, Ni Z, Chen L, Yang L. miR-100-5p-abundant exosomes derived from infrapatellar fat pad MSCs protect articular cartilage and ameliorate gait abnormalities *via* inhibition of mTOR in osteoarthritis. *Biomaterials* 2019; **206**: 87-100 [PMID: 30927715 DOI: 10.1016/j.biomaterials.2019.03.022]
- He L, He T, Xing J, Zhou Q, Fan L, Liu C, Chen Y, Wu D, Tian Z, Liu B, Rong L. Bone marrow mesenchymal stem cell-derived exosomes protect cartilage damage and relieve knee osteoarthritis pain in a rat model of osteoarthritis. *Stem Cell Res Ther* 2020; **11**: 276 [PMID: 32748615 DOI: 10.1038/s41584-020-00518-6]

- 32650828 DOI: [10.1186/s13287-020-01781-w](https://doi.org/10.1186/s13287-020-01781-w)]
- 19 **Xu X**, Liang Y, Li X, Ouyang K, Wang M, Cao T, Li W, Liu J, Xiong J, Li B, Xia J, Wang D, Duan L. Exosome-mediated delivery of kartogenin for chondrogenesis of synovial fluid-derived mesenchymal stem cells and cartilage regeneration. *Biomaterials* 2021; **269**: 120539 [PMID: [33243424](https://pubmed.ncbi.nlm.nih.gov/33243424/) DOI: [10.1016/j.biomaterials.2020.120539](https://doi.org/10.1016/j.biomaterials.2020.120539)]
  - 20 **Liang Y**, Duan L, Lu J, Xia J. Engineering exosomes for targeted drug delivery. *Theranostics* 2021; **11**: 3183-3195 [PMID: [33537081](https://pubmed.ncbi.nlm.nih.gov/33537081/) DOI: [10.7150/thno.52570](https://doi.org/10.7150/thno.52570)]
  - 21 **Wang JY**, Zhang Q, Wang DD, Yan W, Sha HH, Zhao JH, Yang SJ, Zhang HD, Hou JC, Xu HZ, He YJ, Hu JH, Zhong SL, Tang JH. MiR-29a: a potential therapeutic target and promising biomarker in tumors. *Biosci Rep* 2018; **38** [PMID: [29217524](https://pubmed.ncbi.nlm.nih.gov/29217524/) DOI: [10.1042/bsr20171265](https://doi.org/10.1042/bsr20171265)]
  - 22 **Cui Y**, Wang X, Lin F, Li W, Zhao Y, Zhu F, Yang H, Rao M, Li Y, Liang H, Dai M, Liu B, Chen L, Han D, Lu R, Peng W, Zhang Y, Song C, Luo Y, Pan P. MiR-29a-3p Improves Acute Lung Injury by Reducing Alveolar Epithelial Cell PANoptosis. *Aging Dis* 2022; **13**: 899-909 [PMID: [35656115](https://pubmed.ncbi.nlm.nih.gov/35656115/) DOI: [10.14336/AD.2021.1023](https://doi.org/10.14336/AD.2021.1023)]
  - 23 **Dey S**, Udari LM, RiveraHernandez P, Kwon JJ, Willis B, Easler JJ, Fogel EL, Pandol S, Kota J. Loss of miR-29a/b1 promotes inflammation and fibrosis in acute pancreatitis. *JCI Insight* 2021; **6** [PMID: [34464354](https://pubmed.ncbi.nlm.nih.gov/34464354/) DOI: [10.1172/jci.insight.149539](https://doi.org/10.1172/jci.insight.149539)]
  - 24 **Guo Y**, Wu Y, Shi J, Zhuang H, Ci L, Huang Q, Wan Z, Yang H, Zhang M, Tan Y, Sun R, Xu L, Wang Z, Shen R, Fei J. miR-29a/b(1) Regulates the Luteinizing Hormone Secretion and Affects Mouse Ovulation. *Front Endocrinol (Lausanne)* 2021; **12**: 636220 [PMID: [34135859](https://pubmed.ncbi.nlm.nih.gov/34135859/) DOI: [10.3389/fendo.2021.636220](https://doi.org/10.3389/fendo.2021.636220)]
  - 25 **Li X**, Zhen Z, Tang G, Zheng C, Yang G. MiR-29a and MiR-140 Protect Chondrocytes against the Anti-Proliferation and Cell Matrix Signaling Changes by IL-1 $\beta$ . *Mol Cells* 2016; **39**: 103-110 [PMID: [26608362](https://pubmed.ncbi.nlm.nih.gov/26608362/) DOI: [10.14348/molcells.2016.2179](https://doi.org/10.14348/molcells.2016.2179)]
  - 26 **Lu GD**, Cheng P, Liu T, Wang Z. BMSC-Derived Exosomal miR-29a Promotes Angiogenesis and Osteogenesis. *Front Cell Dev Biol* 2020; **8**: 608521 [PMID: [33363169](https://pubmed.ncbi.nlm.nih.gov/33363169/) DOI: [10.3389/fcell.2020.608521](https://doi.org/10.3389/fcell.2020.608521)]
  - 27 **Jin Z**, Ren J, Qi S. Exosomal miR-9-5p secreted by bone marrow-derived mesenchymal stem cells alleviates osteoarthritis by inhibiting syndecan-1. *Cell Tissue Res* 2020; **381**: 99-114 [PMID: [32377874](https://pubmed.ncbi.nlm.nih.gov/32377874/) DOI: [10.1007/s00441-020-03193-x](https://doi.org/10.1007/s00441-020-03193-x)]
  - 28 **Lequesne MG**, Samson M. Indices of severity in osteoarthritis for weight bearing joints. *J Rheumatol Suppl* 1991; **27**: 16-18 [PMID: [2027118](https://pubmed.ncbi.nlm.nih.gov/2027118/)]
  - 29 **Loeser RF**, Collins JA, Diekman BO. Ageing and the pathogenesis of osteoarthritis. *Nat Rev Rheumatol* 2016; **12**: 412-420 [PMID: [27192932](https://pubmed.ncbi.nlm.nih.gov/27192932/) DOI: [10.1038/nrrheum.2016.65](https://doi.org/10.1038/nrrheum.2016.65)]
  - 30 **Wallace IJ**, Worthington S, Felson DT, Jurmain RD, Wren KT, Maijanen H, Woods RJ, Lieberman DE. Knee osteoarthritis has doubled in prevalence since the mid-20th century. *Proc Natl Acad Sci U S A* 2017; **114**: 9332-9336 [PMID: [28808025](https://pubmed.ncbi.nlm.nih.gov/28808025/) DOI: [10.1073/pnas.1703856114](https://doi.org/10.1073/pnas.1703856114)]
  - 31 **Khan HI**, Aitken D, Chou L, McBride A, Ding C, Blizzard L, Pelletier JP, Pelletier JM, Cicuttini F, Jones G. A family history of knee joint replacement increases the progression of knee radiographic osteoarthritis and medial tibial cartilage volume loss over 10 years. *Osteoarthritis Cartilage* 2015; **23**: 203-209 [PMID: [25464166](https://pubmed.ncbi.nlm.nih.gov/25464166/) DOI: [10.1016/j.joca.2014.11.016](https://doi.org/10.1016/j.joca.2014.11.016)]
  - 32 **Roemer FW**, Kwok CK, Hayashi D, Felson DT, Guermazi A. The role of radiography and MRI for eligibility assessment in DMOAD trials of knee OA. *Nat Rev Rheumatol* 2018; **14**: 372-380 [PMID: [29752462](https://pubmed.ncbi.nlm.nih.gov/29752462/) DOI: [10.1038/s41584-018-0010-z](https://doi.org/10.1038/s41584-018-0010-z)]
  - 33 **Xing D**, Kwong J, Yang Z, Hou Y, Zhang W, Ma B, Lin J. Intra-articular injection of mesenchymal stem cells in treating knee osteoarthritis: a systematic review of animal studies. *Osteoarthritis Cartilage* 2018; **26**: 445-461 [PMID: [29427723](https://pubmed.ncbi.nlm.nih.gov/29427723/) DOI: [10.1016/j.joca.2018.01.010](https://doi.org/10.1016/j.joca.2018.01.010)]
  - 34 **Ozeki N**, Muneta T, Koga H, Nakagawa Y, Mizuno M, Tsuji K, Mabuchi Y, Akazawa C, Kobayashi E, Matsumoto K, Futamura K, Saito T, Sekiya I. Not single but periodic injections of synovial mesenchymal stem cells maintain viable cells in knees and inhibit osteoarthritis progression in rats. *Osteoarthritis Cartilage* 2016; **24**: 1061-1070 [PMID: [26880531](https://pubmed.ncbi.nlm.nih.gov/26880531/) DOI: [10.1016/j.joca.2015.12.018](https://doi.org/10.1016/j.joca.2015.12.018)]
  - 35 **Kim JE**, Lee SM, Kim SH, Tatman P, Gee AO, Kim DH, Lee KE, Jung Y, Kim SJ. Effect of self-assembled peptide-mesenchymal stem cell complex on the progression of osteoarthritis in a rat model. *Int J Nanomedicine* 2014; **9** Suppl 1: 141-157 [PMID: [24872709](https://pubmed.ncbi.nlm.nih.gov/24872709/) DOI: [10.2147/IJN.S54114](https://doi.org/10.2147/IJN.S54114)]
  - 36 **Yang X**, Zhu TY, Wen LC, Cao YP, Liu C, Cui YP, Meng ZC, Liu H. Intraarticular Injection of Allogenic Mesenchymal Stem Cells has a Protective Role for the Osteoarthritis. *Chin Med J (Engl)* 2015; **128**: 2516-2523 [PMID: [26365972](https://pubmed.ncbi.nlm.nih.gov/26365972/) DOI: [10.4103/0366-6999.164981](https://doi.org/10.4103/0366-6999.164981)]
  - 37 **Tang Y**, Pan ZY, Zou Y, He Y, Yang PY, Tang QQ, Yin F. A comparative assessment of adipose-derived stem cells from subcutaneous and visceral fat as a potential cell source for knee osteoarthritis treatment. *J Cell Mol Med* 2017; **21**: 2153-2162 [PMID: [28374574](https://pubmed.ncbi.nlm.nih.gov/28374574/) DOI: [10.1111/jcmm.13138](https://doi.org/10.1111/jcmm.13138)]
  - 38 **Gupta PK**, Chullikana A, Rengasamy M, Shetty N, Pandey V, Agarwal V, Wagh SY, Vellotare PK, Damodaran D, Viswanathan P, Thej C, Balasubramanian S, Majumdar AS. Efficacy and safety of adult human bone marrow-derived, cultured, pooled, allogeneic mesenchymal stromal cells (Stempeucel®): preclinical and clinical trial in osteoarthritis of the knee joint. *Arthritis Res Ther* 2016; **18**: 301 [PMID: [27993154](https://pubmed.ncbi.nlm.nih.gov/27993154/) DOI: [10.1186/s13075-016-1195-7](https://doi.org/10.1186/s13075-016-1195-7)]
  - 39 **Gao B**, Gao W, Wu Z, Zhou T, Qiu X, Wang X, Lian C, Peng Y, Liang A, Qiu J, Zhu Y, Xu C, Li Y, Su P, Huang D. Melatonin rescued interleukin 1 $\beta$ -impaired chondrogenesis of human mesenchymal stem cells. *Stem Cell Res Ther* 2018; **9**: 162 [PMID: [29898779](https://pubmed.ncbi.nlm.nih.gov/29898779/) DOI: [10.1186/s13287-018-0892-3](https://doi.org/10.1186/s13287-018-0892-3)]
  - 40 **Zhen G**, Wen C, Jia X, Li Y, Crane JL, Mears SC, Askin FB, Frassica FJ, Chang W, Yao J, Carrino JA, Cosgarea A, Artemov D, Chen Q, Zhao Z, Zhou X, Riley L, Sponseller P, Wan M, Lu WW, Cao X. Inhibition of TGF- $\beta$  signaling in mesenchymal stem cells of subchondral bone attenuates osteoarthritis. *Nat Med* 2013; **19**: 704-712 [PMID: [23685840](https://pubmed.ncbi.nlm.nih.gov/23685840/) DOI: [10.1038/nm.3143](https://doi.org/10.1038/nm.3143)]
  - 41 **Bornes TD**, Adesida AB, Jomha NM. Mesenchymal stem cells in the treatment of traumatic articular cartilage defects: a comprehensive review. *Arthritis Res Ther* 2014; **16**: 432 [PMID: [25606595](https://pubmed.ncbi.nlm.nih.gov/25606595/) DOI: [10.1186/s13075-014-0432-1](https://doi.org/10.1186/s13075-014-0432-1)]
  - 42 **Liu Y**, Lin L, Zou R, Wen C, Wang Z, Lin F. MSC-derived exosomes promote proliferation and inhibit apoptosis of chondrocytes *via* lncRNA-KLF3-AS1/miR-206/GIT1 axis in osteoarthritis. *Cell Cycle* 2018; **17**: 2411-2422 [PMID: [30324848](https://pubmed.ncbi.nlm.nih.gov/30324848/) DOI: [10.1080/15384101.2018.1526603](https://doi.org/10.1080/15384101.2018.1526603)]
  - 43 **Xiao X**, Xu M, Yu H, Wang L, Li X, Rak J, Wang S, Zhao RC. Mesenchymal stem cell-derived small extracellular vesicles mitigate oxidative stress-induced senescence in endothelial cells *via* regulation of miR-146a/Src. *Signal Transduct Target Ther* 2021; **6**: 354 [PMID: [34675187](https://pubmed.ncbi.nlm.nih.gov/34675187/) DOI: [10.1038/s41392-021-00765-3](https://doi.org/10.1038/s41392-021-00765-3)]



Published by **Baishideng Publishing Group Inc**  
7041 Koll Center Parkway, Suite 160, Pleasanton, CA 94566, USA  
**Telephone:** +1-925-3991568  
**E-mail:** [office@baishideng.com](mailto:office@baishideng.com)  
**Help Desk:** <https://www.f6publishing.com/helpdesk>  
<https://www.wjgnet.com>

